**Supplemental Information**

*5'UTR Structure Information:* The HCV 5'-UTR is composed of four domains (D-I through D-IV, Fig. 3a). The two miRNA target sites (S1 and S2) occur in the region between domains I (D-I) and II (D-II). Domains II-IV define the HCV internal ribosome entry site (IRES) (6). The most accurate data on the secondary structure of the 5'-UTR come from NMR and crystallographic studies of domain II and portions of domain III (13); (Supplemental Fig. 2a). As noted by Dr. Puglisi and colleagues (14), the enzymatic mapping of DI-DII resulted in considerable inaccuracies, as evident by comparing the NMR-derived structure to the original enzymatically determined D-I/D-II structure (3) (Supplemental Fig. 2c,d). In contrast, sf-SHAPE resulted in a secondary structure consistent with the NMR data; consistent with the high accuracy of SHAPE over enzymatic methods (4).

We did note two minor exceptions from the structural data at NT 67 (Domain II) and NTs 227-229 (Domain III, junction of subdomains a, b, and c). These nucleotides were found by sf-SHAPE to be flexible. In the Domain II NMR structure (14), NT 67 is base-paired. An explanation for this discrepancy might be that the NMR structure at this region was solved using two separate RNA constructs, which notably overlapped at this region. An explanation for the discrepancy at NTs 227-229, which in the crystal structure of the 4-way junction of domain III are base-paired, may be that sf-SHAPE is performed in solution and/or the minor sequence differences in the crystal structure construct play a role in the observed differences (11).

As stated in the primary communication, we were unable to resolve the state of NTs 17-28, which includes the first (S1) miR-122 target site. This was due to a high background of reverse transcriptase (RT) pause sites. Although we cannot rule out that the latter are the result of context-specific degradation, we consider structure-induced pausing (5) to be an equally likely possibility for the following reason: mutation of the S1 sequence eliminates these pauses and permits RT read-through. Studies to further investigate this possibility are on-going.

With regard to those areas of the HCV 5'-UTR for which crystal structure or NMR data is not available, we note the following differences with respect to prior secondary structure models generated by traditional enzymatic mapping methods: (a) instead of the extended loop originally proposed for domain IIIb (3) our data is more consistent with a 3 BP helix and two small loops; and (b) we propose a smaller domain IV stem, which does not include base-pairings of NTs 331-332 with 353-354 (8). This is consistent with prior mutagenesis that did not show a significant effect of disrupting these two nucleotides on *in vivo* translation (8). Additional and more extensive mutagenesis will certainly be required to validate these differences.

*Additional Experimental Details:* 2' acylation with NMIA (19) and Reverse transcription (RT) primer extension were performed at 45°Cx1', 52°Cx25', 65°Cx5', as previously described (16). Exceptions were as follows: (a) RNA purification after acylation as well as removal of miRNA before RT (as appropriate), was performed using RNA C&C columns (Zymoresearch), rather than ethanol precipitation; (b) before and after SHAPE primer buffer was added, the mixture was placed at room temperature for 2-5 min, which enhanced RT transcription yields *significantly*; (c) DNA purification was

performed using Sephadex G-50 size exclusion resin in 96-well format then concentrated by vacuum centrifugation, resulting in a more significant removal of primer; and (d) 1 pmol rather than 3 pmol of RNA was used in ddGTP RNA sequences reactions.

With respect to the miR-122 experiments, using 10 or 100x of the miRNA (over the HCV RNA concentration) made no significant difference to the resultant structures; and no difference was apparent if the 5'UTR was folded with microRNA-122 or before its addition.

*PeakScanner* parameters were set to the following parameters: smoothing=none; window size=25; size calling=local southern; baseline window=51; peak threshold=15. Fragments 250 and 340 were computationally excluded from the ROX500 standard (1). RNAstructure parameters: slope and intercept parameters of 2.6 and -0.8 kcal/mol, were initially tried, as suggested (4); however, we found that smaller intercepts closer to 0.0 kcal/mol (e.g. ~ -0.3) produced fewer less optimal structures. We speculate that this minor parameter difference may be due to the precise fitting achieved between experimental and control data sets by the automated FAST algorithm.

*InStat 3* (Graphpad) was used for statistical analysis of the miRNA mutant experiments, as follows: first, reactivity data for each nucleotide position, as a function of the different miR-122 mutants, was examined by one-way ANOVA. NTs 29 and 43-45 were not found to have statistically significant variations in reactivity, likely due to the low reactivity of these nucleotides even in the absence of miR-122. NTs 30-42 were found to have statistically significant variations in their SHAPE reactivity. The SHAPE reactivities for these nucleotides (30-42) were then further analysed by individual comparison of all mutant-specific SHAPE reactivities to WT miR-122 (reference), using the Tukey-Kramer Multiple Comparisons Test. Boxes with an (*) indicate values that are statistically different (p-values < 0.001) from the SHAPE reactivity determined in the presence of WT miR-122 (r). The miR-122 bound state was chosen as the reference because statistical deviations from this suggest a gain of flexibility due to disruption of base-pairing or loss of other constraints. Statistical analysis of replication and translation was by one-way ANOVA and subsequent Tukey-Kramer Multiple Comparisons Test. SHAPE reactivity-base stacking comparisons were made using the more conservative nonparametric ANOVA (Kruskal-Wallis Test), due to the non-normal distribution of SHAPE reactivities.

*Materials:* Materials for sf-SHAPE were as described for SHAPE (18, 19), except only the single fluorophore 6FAM was used for all labeled primers. The PCR template for the GN1b/con1 5'UTR construct was generated from Bart79I (2). The PCR template for the GN2/J6 5'UTR construct was generated from HCVcc (12). The self-replicating HCV construct (J6/JFH1) with a luciferase reporter was as described previously (17). All constructs were originally kind gifts of Dr. Charles Rice.

RNAs were generated by *in-vitro* transcription, using T7 MEGAscript. RNAs for SHAPE were purified by MEGAclear, with purity and length verified by capillary electrophoresis. RNAs which were transfected were purified by LiCl precipitation, with purity and length verified by agarose gel electrophoresis.

With respect to the rescue experiments, prior rescue experiments using mutant miR-122s did not require mutation of the star strand, only the non-star strand (7, 9, 10). For this tested tail interaction, we found that HCV replication rescue was far greater (~4x

vs. ~2x) when both the non-star and star strands contained the appropriate compensatory mutations (see supplementary information for all sequence information). This was also found to be the case by the Sarnow group (15).

OLIGOS/microRNA:

miR-122: UGGAGUGUGACAAUGGUGUUUG
miR-124: UAAGGCACGCGGUGAAUGCC
122Mut1: UGGAGUGUGACAA
122Mut2: UGGAGUGUGACAAGAAUGCC
122Mut3: UGGAGUGCGCGGUUGGUGUUUG
122Mut4: UGGAGUGUGACAAUGGUGUGGC
122Mut5: UGGAGUGUGACAAUGUGGUUUG

miR-122 duplex (exogenous supplementation):
Non-Star: UGGAGUGUGACAAUGGUGUUUGU
Star Strand: AAACGCCAUUAUCACACUAAAUA

P3mir-122 duplex (exogenous supplementation)

P3-122: UG**C**AGUGUGACAAUGGUGUUUGU
Star strand: AAACGCCAUUAUCACACUAAAUA

P3-122 Mut1 : UG**C**AGUGUGACAA
P3-122 Mut1* : AUCACACUAAAUA

P3-122 Mut2 : UG**C**AGUGUGACAA**GAAUGCC**
P3-122 Mut2* : **CAUUC**UUAUCACACUAAAUA

P3-122 Mut3 : UG**C**AGUG**CGCGGU**UGGUGUUUGU
P3-122 Mut3* : AAACGCCA**ACAGCG**CACUAAAUA

P3-122 Mut4 : UG**C**AGUGUGACAAUGGUGU**GGC**U
P3-122 Mut4* : **CC**ACGCCAUUAUCACACUAAAUA

P3-122 Mut5 : UG**C**AGUGUGACAAUG**GU**GUUUGU
P3-122 Mut5* : AAAC**CG**CAUUAUCACACUAAAUA

miR-122 G15C mutant duplex (exogenous supplementation):
Non-Star: UGGAGUGUGACAAU**C**GUGUUUGU
Star Strand: AAAC**G**CGAUUAUCACACUAAAUA

miR-124 duplex (exogenous supplementation)
Non-Star: UUAAGGCACGCGGUGAAUGCCA
Star Strand: CCGUGUUCACAGCGGACCUUGA

4-thio-uridine substituted miR-122 (Z=4-thio-uridine):
MIR122-TU1: UGGAGUGUGACAAZGGUGUUUG
MIR122-TU2: UGGAGUGUGACAAUGGZGUUUG
MIR122-TU3: UGGAGUGUGACAAUGGUGZUUG
MIR122-TU4: UGGAGZGUGACAAUGGUGUUUG

OLIGOS/DNA:

sf-SHAPE primers:

Genotype1: 6FAM-CCAGGCATTG AGCGGGTTGA TCCAAG (5′ half of 5′UTR)
6FAM-CCTGCGTGCA ATCCATCTTG (3′ half of 5′UTR)
Genotype2: 6FAM-CGGGCATAGAGTGGGTTTATCCAAG (5′ half of 5′UTR)
6FAM-GCCCGGAAACTTAACGTCTTG (3′ half of 5′UTR)

Primers used to generate DNA templates for RNA transcription:

Genotype1: Forward: GTCTGACGCTC AGTGGAACGA AAACTCACG
Reverse: CCTGCGTGCA ATCCATCTTG TTCAATCATG
Genotype2: Forward: CATTCAGGCT GCGCAACTGTTG
Reverse: GACAGCATTA CCTGGCAGCTCC

Mutagenesis by PCR:

Site1Mutant:
Forward: GGAAGGAAGGAAGAGATAAT ACGACTCACTATAGCCAGCC CCCGATTGGG
GGCGAACAAAAACCATAGAT CACTCCCCTGTGAGGAACTAC
Reverse: CCTGCGTGCA ATCCATCTTG TTCAATCATG

Site2Mutant:
Forward: GGAAGGAAGGAAGAGATAAT ACGACTCACTATAGCCAGCC
CCCGATTGGGGGCGACACTC CACCATAGATTGCCTTCCTG
TGAGGAACTACTGTCTTCACGCAG
Reverse: CCTGCGTGCA ATCCATCTTG TTCAATCATG

Delta(1-44):
Forward: GGAAGGAAGGAAGAGATAAT ACGACTCACTATAGCCTGTG
AGGAACTACTGTCTTCACGCAG
Reverse: CCTGCGTGCA ATCCATCTTG TTCAATCATG

C31G Mutagenesis by QuickChange Lightening (Stratagene):

CAGTAGTTCCTCACAGGGGAGTGATTCATCGCGGAGTGTCGC
GCGACACTCCGCGATGAATCACTCCCCTGTGAGGAACTACTG

## Supplemental Figure 1

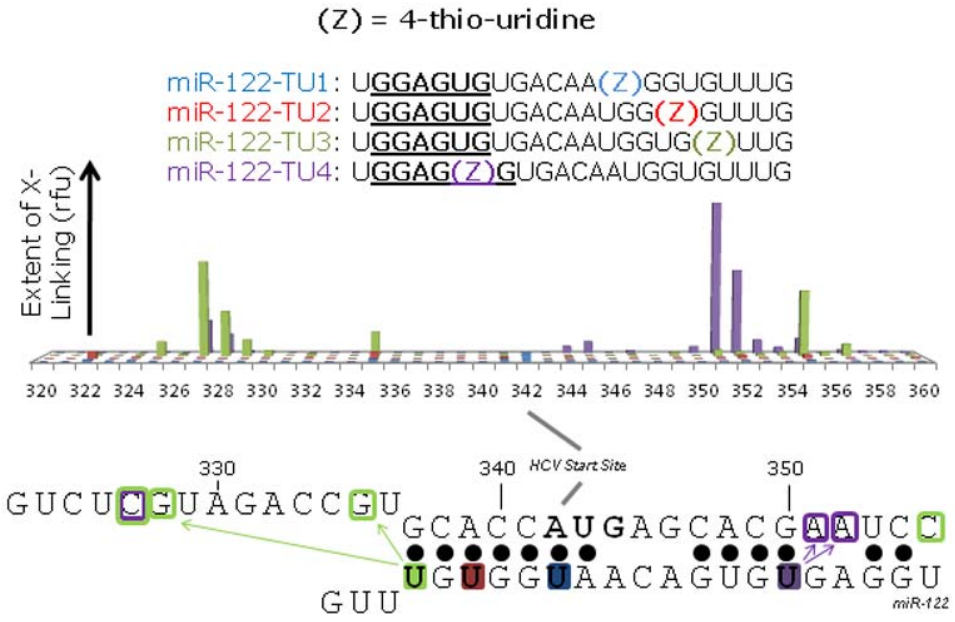


**Supplemental Figure 1.** 4-Thio-Uridine substituted variants of miR-122 were added to a solution of the folded ΔNT1-44 5'UTR construct – to ensure that any binding that was observed would be independent of S1 and S2. UV cross-linking was then performed as described in Sontheimer et al., 1994. The location of cross-linking sites were determined by primer extension/reverse transcription. Fragments were separated by capillary electrophoresis, and analyzed using the FAST program. Although the extent of cross-linking cannot be directly compared between different thio-uridine constructs (Sontheimer et al., 1994), the respective location of the cross-links between miR-122 and HCV domain IV are consistent with the proposed base-pairings. To date, however, mutagenesis studies to functionally confirm the relevance of this interaction have been negative. Experiments to investigate the role of this interaction for other aspects of the viral life cycle are ongoing.

## Supplemental Figure 2

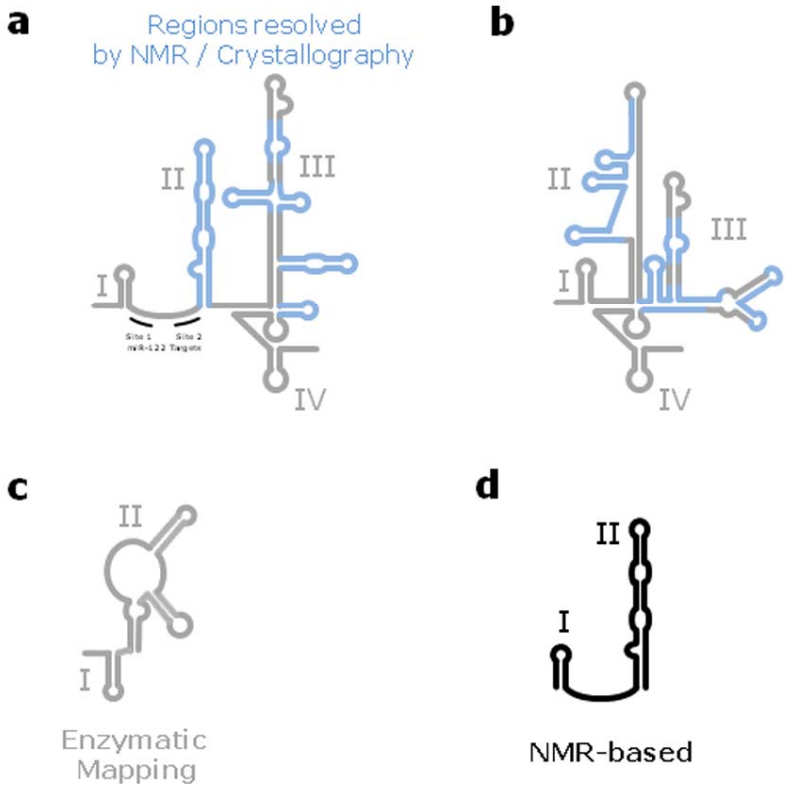


**Supplemental Figure 2. Current and prior proposed structures of HCV 5'UTR. a**. Secondary structure resulting from SHAPE analysis. Regions for which gold-standard crystallographic or NMR structure data is available are indicated in light blue (note the very high concordance between the SHAPE-derived and gold standard structures, as indicated in Figure 1 of the main text). The two miR-122 target sites are found between domains I and II. **b.** Secondary structure solved by RNAstructure without SHAPE data (note the difference SHAPE makes, especially in the gold-standard regions). **c.** Original secondary structure proposed for DI-DII, as determined by enzymatic mapping. **d.** The revised secondary structure after incorporation of NMR data.

1. **Akbari, A., G. Marthinsen, J. T. Lifjeld, F. Albregtsen, L. Wennerberg, N. C. Stenseth, and K. S. Jakobsen.** 2008. Improved DNA fragment length estimation in capillary electrophoresis. Electrophoresis **29:**1273-85.
2. **Blight, K. J., A. A. Kolykhalov, and C. M. Rice.** 2000. Efficient initiation of HCV RNA replication in cell culture. Science **290:**1972-4.
3. **Brown, E. A., H. Zhang, L. H. Ping, and S. M. Lemon.** 1992. Secondary structure of the 5' nontranslated regions of hepatitis C virus and pestivirus genomic RNAs. Nucleic Acids Res **20:**5041-5.
4. **Deigan, K. E., T. W. Li, D. H. Mathews, and K. M. Weeks.** 2009. Accurate SHAPE-directed RNA structure determination. Proc Natl Acad Sci U S A **106:**97-102.
5. **Ehresmann, C., F. Baudin, M. Mougel, P. Romby, J. P. Ebel, and B. Ehresmann.** 1987. Probing the structure of RNAs in solution. Nucleic Acids Res **15:**9109-28.
6. **Fraser, C. S., and J. A. Doudna.** 2007. Structural and mechanistic insights into hepatitis C viral translation initiation. Nat Rev Microbiol **5:**29-38.
7. **Henke, J. I., D. Goergen, J. Zheng, Y. Song, C. G. Schuttler, C. Fehr, C. Junemann, and M. Niepmann.** 2008. microRNA-122 stimulates translation of hepatitis C virus RNA. Embo J **27:**3300-10.
8. **Honda, M., E. A. Brown, and S. M. Lemon.** 1996. Stability of a stem-loop involving the initiator AUG controls the efficiency of internal initiation of translation on hepatitis C virus RNA. Rna **2:**955-68.
9. **Jangra, R. K., M. Yi, and S. M. Lemon.** 2010. Regulation of hepatitis C virus translation and infectious virus production by the microRNA miR-122. J Virol **84:**6615-25.
10. **Jopling, C. L., M. Yi, A. M. Lancaster, S. M. Lemon, and P. Sarnow.** 2005. Modulation of hepatitis C virus RNA abundance by a liver-specific MicroRNA. Science **309:**1577-81.
11. **Kieft, J. S., K. Zhou, A. Grech, R. Jubin, and J. A. Doudna.** 2002. Crystal structure of an RNA tertiary domain essential to HCV IRES-mediated translation initiation. Nat Struct Biol **9:**370-4.
12. **Lindenbach, B. D., M. J. Evans, A. J. Syder, B. Wolk, T. L. Tellinghuisen, C. C. Liu, T. Maruyama, R. O. Hynes, D. R. Burton, J. A. McKeating, and C. M. Rice.** 2005. Complete replication of hepatitis C virus in cell culture. Science **309:**623-6.
13. **Lukavsky, P. J.** 2009. Structure and function of HCV IRES domains. Virus Res **139:**166-71.
14. **Lukavsky, P. J., I. Kim, G. A. Otto, and J. D. Puglisi.** 2003. Structure of HCV IRES domain II determined by NMR. Nat Struct Biol **10:**1033-8.
15. **Machlin, E. S., P. Sarnow, and S. M. Sagan.** 2011. Masking the 5' terminal nucleotides of the hepatitis C virus genome by an unconventional microRNA-target RNA complex. Proc Natl Acad Sci U S A.
16. **Mortimer, S. A., and K. M. Weeks.** 2009. Time-resolved RNA SHAPE chemistry: quantitative RNA structure analysis in one-second snapshots and at single-nucleotide resolution. Nat Protoc **4:**1413-21.

17. **Tscherne, D. M., C. T. Jones, M. J. Evans, B. D. Lindenbach, J. A. McKeating, and C. M. Rice.** 2006. Time- and temperature-dependent activation of hepatitis C virus for low-pH-triggered entry. J Virol **80:**1734-41.
18. **Wilkinson, K. A., R. J. Gorelick, S. M. Vasa, N. Guex, A. Rein, D. H. Mathews, M. C. Giddings, and K. M. Weeks.** 2008. High-throughput SHAPE analysis reveals structures in HIV-1 genomic RNA strongly conserved across distinct biological states. PLoS Biol **6:**e96.
19. **Wilkinson, K. A., E. J. Merino, and K. M. Weeks.** 2006. Selective 2'-hydroxyl acylation analyzed by primer extension (SHAPE): quantitative RNA structure analysis at single nucleotide resolution. Nat Protoc **1:**1610-6.